

ISSN 2410-6593 (Print), ISSN 2686-7575 (Online)

<https://doi.org/10.32362/2410-6593-2020-15-2-7-20>

UDC 535.012.2



Photoalignment and photopatterning: New liquid crystal technology for displays and photonics

Vladimir G. Chigrinov

School of Physics and Optoelectronic Engineering, Foshan University, Foshan, 528000 Peoples Republic of China

@Corresponding author, e-mail: eechigr@ust.hk

Objectives. Since the end of the 20th century, liquid crystals have taken a leading position as a working material for the display industry. In particular, this is due to the advances in the control of surface orientation in thin layers of liquid crystals, which is necessary for setting the initial orientation of the layer structure in the absence of an electric field. The operation of most liquid crystal displays is based on electro-optical effects, arising from the changes in the initial orientation of the layers when the electric field is turned on, and the relaxation of the orientation structure under the action of surfaces after the electric field is turned off. In this regard, the high quality of surface orientation directly affects the technical characteristics of liquid crystal displays. The traditional technology of rubbing substrates, currently used in the display industry, has several disadvantages associated with the formation of a static charge on the substrates and surface contamination with microparticles. This review discusses an alternative photoalignment technology for liquid crystals on the surface, using materials sensitive to polarization of electromagnetic irradiation. Also, this review describes various applications of photosensitive azo dyes as photo-oriented materials.

Results. The alternative photoalignment technology, which employs materials sensitive to electromagnetic polarization, allows to create the orientation of liquid crystals on the surface without mechanical impact and to control the surface anchoring force of a liquid crystal. This provides the benefits of using the photoalignment technology in the display industry and photonics—where the use of the rubbing technology is extremely difficult. The optical image rewriting mechanism is discussed, using electronic paper with photo-inert and photoaligned surfaces as an example. Further, different ways of using the photoalignment technology in liquid crystal photonics devices that control light beams are described. In particular, we consider switches, controllers and polarization rotators, optical attenuators, switchable diffraction gratings, polarization image analyzers, liquid crystal lenses, and ferroelectric liquid crystal displays with increased operation speed.

Conclusions. The liquid crystal photoalignment and photopatterning technology is a promising tool for new display and photonics applications. It can be used for light polarization rotation; voltage controllable diffraction; fast switching of the liquid crystal refractive index; alignment of liquid crystals in super-thin photonic holes, curved and 3D surfaces; and many more applications.

Keywords: electro-optical effects in liquid crystals, liquid crystals in fiber optics, liquid crystal surface alignment, optical elements and materials for liquid crystal devices.

For citation: Chigrinov V.G. Photoalignment and photopatterning: New liquid crystal technology for displays and photonics. *Tonk. Khim. Tekhnol. = Fine Chem. Technol.* 2020;15(2):7-20. <https://doi.org/10.32362/2410-6593-2020-15-2-7-20>

Фотоориентация и фотопаттернинг: Новая жидкокристаллическая технология для дисплеев и фотоники

В.Г. Чигринов

Школа физики и оптоэлектронного инжиниринга, Фошаньский Университет, Фошань, 528000 Китайская Народная Республика

@Автор для переписки, e-mail: eechigr@ust.hk

Цели. С конца XX века жидкие кристаллы занимают лидирующее положение среди рабочих материалов для дисплейной индустрии. В частности, это стало возможным благодаря достижениям в области управления поверхностной ориентацией в тонких слоях жидких кристаллов, необходимой для задания исходной ориентационной структуры слоя в отсутствие электрического поля. Работа большинства жидкокристаллических дисплеев основана на электрооптических эффектах, возникающих за счет изменения исходной ориентации слоев при включении электрического поля и обратной релаксации ориентационной структуры под действием поверхностей после выключения электрического поля. По этой причине высокое качество поверхностной ориентации напрямую влияет на технические характеристики жидкокристаллических дисплеев. Используемая в настоящее время в дисплейной индустрии традиционная технология натирания подложек имеет ряд недостатков, связанных с образованием на подложках статического заряда и загрязнением поверхности микрочастицами. В данном обзоре рассмотрена альтернативная технология фотоориентации жидких кристаллов на поверхности с использованием материалов, чувствительных к поляризации электромагнитного излучения. Также описаны различные приложения с использованием фоточувствительных азокрасителей в качестве фотоориентируемых материалов.

Результаты. Альтернативная технология фотоориентации позволяет создавать ориентацию жидких кристаллов на поверхности без механического воздействия, а также контролировать силу сцепления жидкого кристалла с поверхностью подложек. Это обеспечивает преимущество использования технологии фотоориентации в дисплейной индустрии и в фотонике, где применение технологии натирания крайне затруднительно. На примере электронной бумаги с фотоинертной и фоточувствительной поверхностями рассмотрен механизм оптической перезаписи изображения. Описаны различные варианты использования технологии фотоориентации в жидкокристаллических устройствах фотоники, обеспечивающих управление световыми пучками. В частности, рассмотрены переключатели, контроллеры и вращатели поляризации, оптические аттенюаторы, переключаемые дифракционные решетки, поляризационные анализаторы изображения, жидкокристаллические линзы, а также ферроэлектрические жидкокристаллические дисплеи с повышенным быстродействием.

Выводы. Технология фотоориентации и фотопаттернинга жидких кристаллов является многообещающей для новых приложений в области дисплеев и фотоники. Технология может быть использована для вращения поляризации света; дифракции, управляемой напряжением; быстрого переключения показателя преломления жидкого кристалла; ориентации жидких кристаллов в супертонких фотонных дырах, на искривленных и 3D поверхностях; и многого другого.

Ключевые слова: электрооптические эффекты в жидких кристаллах, жидкие кристаллы в волоконной оптике, поверхностная ориентация жидких кристаллов, оптические элементы и материалы для жидкокристаллических устройств.

Для цитирования: Chigrinov V.G. Photoalignment and photopatterning: New liquid crystal technology for displays and photonics. *Tonk. Khim. Tekhnol. = Fine Chem. Technol.* 2020;15(2):7-20. <https://doi.org/10.32362/2410-6593-2020-15-2-7-20>

PHOTOALIGNMENT AND PHOTOPATTERNING TECHNOLOGY

The paper presents a comprehensive review of liquid crystal (LC) photoalignment technologies, based on the use of polarization-sensitive (photo-anisotropic) materials with anisotropic substances. Such materials demonstrate photo-induced optical anisotropy (birefringence and dichroism) upon absorbance of polarized (or non-polarized but direct) optical (ultraviolet (UV) or visible) irradiation. The mechanism of this effect can be explained as a result of photochemical mono- or bimolecular reactions, or orientation ordering, of photochemically stable molecules in solid state films. In fact, light–molecule anisotropic interactions have been in the focus of researchers for a long time, and it is still an intriguing topic. These materials have been shown to provide a high-quality alignment of molecules in an LC cell under specific light irradiation.

Over the past two decades, tremendous improvements have been made in the field of photoalignment [1–4]. Photoalignment materials are now commercially available. A number of new applications, apart from the alignment of LC displays (LCDs) and other LC devices, have been proposed and demonstrated. In particular, the use of photoalignment to activate optical elements in optical signal processing and communications is currently a major direction in display and photonics research.

Photopatterning via the advanced photoalignment technology can make a great contribution to the development of new classes of such devices. Photoalignment has obvious advantages over the usual “rubbing” treatment of glass substrates of LC display cells [5, 6]. The potential benefits of such techniques include [7, 8]:

- elimination of electrostatic charge, impurities, and mechanical damage of the surface;
- controllable pretilt angle and anchoring energy of the LC cell, high thermal and UV stability, and ionic purity;
- some advanced applications of LC in optical data processing, fiber communications, holography and many more—where the traditional “rubbing” treatment is impossible because of the high spatial resolution of the processing system, and/or the complicated geometry of the LC cell;
- capability of efficient LC alignment on flexible and curved substrates;
- manufacturing of new optical elements, e.g., patterned phase retarders and polarizers, tunable optical filters, polarization-insensitive optical lenses with electrically controlled focal length, *etc.*

In this review, we will analyze different applications of photoalignment and photopatterning

based on azo dye layers. We will also discuss certain new applications of the photoalignment technology, including optically rewritable E-paper (ORW), and certain LC photonics devices, such as LC switches, polarization controllers and polarization rotators, variable optical attenuators, photonic crystal fibers filled with LC, switchable diffraction gratings, LC sensors, electrically tunable LC q-plates, LC optical elements with integrated Pancharatnam–Berry phases, fast ferroelectric LCs, and new, highly efficient photovoltaic, optoelectronic, and photonic devices.

OPTICALLY REWRITABLE LIQUID CRYSTAL ALIGNMENT

Traditionally, most approaches in LC E-paper were based on photo-degradation [9, 10] and photocrosslinking mechanisms [11], thus the erasing and writing capabilities of photoalignment films were very limited [7, 12]. The only reversible writing and erasing process can be achieved by the photoalignment in solid films observed in sulfonic azo dye SD1 layers, explained in our pioneering work on its diffusion model [7, 12]. Optical LC alignment can be considered as rewritable, even though it encounters the complete image decay due to the exposure under direct sunlight, the image can be facily restored or changed through a rewriting cycle via a specific exposure device. Photo-stability requirements of such optically rewriteable LC cells are practically diminished, since a display unit does not undergo reversible changes. The optically rewritable technology is a modified method of azo dye based photoalignment, which possesses a considerably high azimuthal anchoring energy, and has a unique feature of reversible in-plane reorientation via photoalignment—photosensitive molecules tend to reorient perpendicular to the polarization of incident light. Typically, an ORW LC cell is comprised of two substrates with different alignment materials (Fig. 1).

One aligning material is optically passive and keeps the alignment direction on one substrate. The other aligning material is optically active and can change its alignment direction after exposure to polarized light through the substrate. In comparison with electrically controlled plastic displays, ORW is significantly thinner, and does not require transparent conductive electrodes, thus indium tin oxide photolithography and etching on a plastic substrate are not needed. By controlling the alignment direction of the photoalignment azo dye layer, which is insoluble in the LC, the switching and continuous gray scale can be achieved. Hence, one can reach the transmission level that corresponds to the specified twist angle of LC in the ORW cell under the initial configuration of

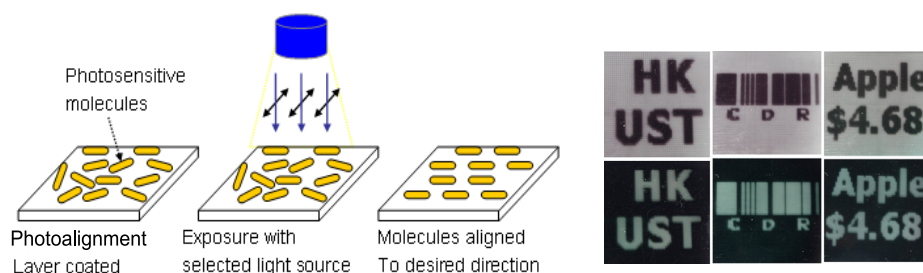


Fig. 1. Left to right: operation mechanism of ORW LC cell—an azo dye photoalignment film rotates its alignment direction in-plane, and eventually reorients perpendicular to the polarization of the writing beam; LC molecules are switched between homogeneous and twisted states controlled by the top photoalignment direction; images of ORW samples.

the polarizers. The tolerance of the cell gap variation of the ORW is very high, as no obvious change in LC transmission is observed when the cell gap changes by 50%, and the achromatic switching of all grey levels in ORW can be achieved [7, 12]. Each transmission level is stable, and the visualization of information on the ORW requires zero power consumption for a long time.

Due to the recent developments in ORW LCD and progress in LC photoalignment, it is possible to separate the E-paper display unit and the driving optoelectronic part, and a significant reduction in the complexity of the ORW E-paper structure makes both devices as cheap as paper [7, 12]. Thus, ORW E-paper is durable, economical and flexible. More research on ORW has revealed that a cheap and low power consuming, highly efficient blue light-emitting diode (LED) can be used as an alternative exposure light source, instead of expensive and highly consuming mercury lamps or lasers. The prototype of the ORW E-paper with the device structure based on a polarizer and plastic substrates was experimentally implemented [12] (Fig. 2).



Fig. 2. ORW E-paper in plastic substrates is highly resistant to mechanical pressure [12].

This prototype uses the optically rewritable alignment technology, and possesses a grey scale capability; it is truly stable, has no electrodes and does not require electric power to display the image with high contrast and wide viewing angles. Nowadays, a new function of the ORW E-paper based on the LC technology, has been developed: it can be used for displaying 3D images to enrich the performance of the single-side light printable ORW E-paper, which was originally designed for 2D images [7, 12].

The light-sensitive photoalignment materials and LC layers were developed to fulfill the following requirements [12]: optical writing/erasing time <2 s; energy of the writing beam <1 J/cm²; more than 1000 reversible cycles; blue LED used as exposure light source. Because of the insufficient durability of contact bonding and the flexible conductor, E-paper displays have the issue of high complexity of the driving electronics. Therefore, an optically rewritable technique is highly desirable. The merits of the ORW E-paper include: no current-conducting layer; no drivers; high tolerance to layer thickness; low manufacturing cost (the price of the ORW E-paper is approximately equal to the price of two polarizers, i.e., around 20 USD/m²). Due to the plastic substrates, the ORW E-paper, as a pioneering innovation in LCD E-paper, exhibits the outstanding flexibility characteristics, and will easily find its place on the market. Some possible applications of the ORW E-paper include light re-printable paper, labels, plastic card displays, 3D paper for security applications, and many more (Fig. 3).



Fig. 3. Left to right: ORW E-paper for advertisements, plastic cards and security applications.

APPLICATION OF PHOTOALIGNMENT IN PHOTONIC LC DEVICES

LC photonic devices based on the photoalignment materials, including passive elements for fiber optical communication used in the fiber-to-the-home (FTTH) program, are becoming increasingly important. FTTH is a form of fiber optical delivery where the fiber extends from the central office to the subscriber's working or living space. Since the Gigabit and Terabit Ethernet can be efficiently used, configurations that bring the fiber right into a building can offer the highest speeds of voice, video, and data delivery. Fast-switching photoaligned LC cells, with microsecond and sub-microsecond switching time, have the potential to replace the currently used micro-electro-mechanical (MEM) switching devices in FTTH systems, with millisecond switching time [13].

The reliable passive optical components are still in high demand, and this trend will continue to grow for a long time. Some LC components, such as LC-based polarization controllers, phase retarders, and coaxial variable optical attenuators have already appeared on the market^{1,2}. For example, a USA-based company Vescent Photonics announced that LC waveguides could be a great electro-optic technology platform for various applications, such as beam steerers, interferometers, lasers, tunable filters, *etc.*³.

Further investigations on passive LC elements for fiber optical communication systems are needed. Silicon photonic devices (high-quality LC switches, voltage controllable filters, and variable optical attenuators) and photoalignment LC devices (e.g., polarization rotators and controllers) are to be developed. New prototypes for packaging are highly desired. New LC materials for fiber optical communications that work in the infrared (IR) range need to be tested. LC tunable sensors, including those based on complementary metal-oxide-semiconductor (CMOS) and LC lenses, are becoming very important for LC photonic applications.

LC switches

Switches for optical fiber networks are becoming more and more important. LC switches have certain advantages compared to MEM switches that are on

commonly used for this purpose, for instance: (i) fast-switching time; (ii) low power consumption and controlling voltages; (iii) high reliability and durability [13]. Nevertheless, the characteristics of thermal drift and wavelength-dependent response time of LC switches should be avoided. We have investigated several LC electro-optical modes, which can be utilized for manufacturing LC switches for optical fiber networks [14].

1. LC switches can make use of the effect of total internal reflection in nematic LC [14]. The total internal reflection switch operates only in the transverse electric mode, and the most promising approach is based on the vertical aligned nematic configuration, realized by photoalignment. The switching time of 1 ms can be easily achieved at the switching pulse amplitude of 5 V [14].

2. A bypass optical switch based on two nematic LC (NLC) cells with the switching time $<200 \mu\text{s}$ was created from two temperature-stabilized photoaligned (NLC) cells [15]. Two subsequent NLC cells with mutually orthogonal optical axes compensate the relaxation of NLC birefringence when they are turned off simultaneously. Thus, the switching time of the two-cell switch can be as short as the turn-on time of the NLC cell. NLC cells can be designed for a certain fiber wavelength by adjusting the cell gap thickness.

3. An LC switch can be designed to control the light propagation in the plane of LC layers [16]. It was experimentally demonstrated that the propagation of the light beam can be noticeably changed by refraction and reflection of light at the sharp boundaries between the regions with different LC orientations induced by photoalignment. LC switches can be electrically controlled. Certain methods were proposed for optimizing the insertion loss and crosstalk of the 1×2 switch for practical photonic applications. It is possible to create an $N \times M$ switch and various optical processing data elements (e.g., attenuators) by using different photoalignment templates. There are many ways to optimize such types of LC devices, and employment of fast-operating ferroelectric liquid crystal layers is one of these approaches, which can provide the microsecond-level operation time.

Polarization controllers and polarization rotators, variable optical attenuators

Polarization controllers are optical elements that can convert an arbitrary input state of polarization (SOP) to a desired one, thus governing the unpredictable polarization change that stems from the polarization-dependent components of the optical fiber system. These optical elements can be made of three successively placed LC cells, which utilize the electrically controlled birefringence to modify the evolution of the SOP [17]. The switching time typically

¹Manufacturers of Innovative of Fiber Optics Components. Lightwaves2020 [Internet]. Milpitas, CA, USA: Lightwaves2020 Inc.; 2020 [Accessed January 15, 2020]. Available from: <http://www.lightwaves2020.com>

²Precision Electro-Optic and Laser Technologies. Vescent Photonics [Internet]. Golden, CO, USA: Vescent Photonics; 2020 [Accessed January 15, 2020]. Available from: <https://www.vescent.com>

³Precision Electro-Optic and Laser Technologies. Vescent Photonics [Internet]. Golden, CO, USA: Vescent Photonics; 2020 [Accessed January 15, 2020]. Available from: <https://www.vescent.com>

the depends LC material, and is around 10 ms for the wavelength of 1.3 μm [17].

A polarization rotator is an optical element that can rotate the linear polarization of the input light to any desired polarization plane. The configuration of our proposed LC polarization rotator comprises a polarizer and two LC homogeneous cells, placed in such a way that their optical axes are at an angle of 45° to each other. One LC cell provides a voltage controllable phase change, and the other is fixed as a quarter wave plate [12]. Such optical element can rotate the light polarization state at any angle between 0° and 90° , depending on the voltage.

LC variable optical attenuators (VOA) typically have the attenuation range of 30 dB for the applied voltage of 12 V in the wavelength range between 1525 and 1575 nm [13], with the response time of approximately 10–30 ms. Some of these attenuators are dependent on the light scattering of a polymer network (PN) filled LC (PN-LC) cell. Due to the refractive index mismatching of the polymer and the LC in the absence of driving voltage, the light from the input fiber is scattered, and it can pass mostly through the PN-LC layer, because of the refractive index match of the polymer and the LC in the presence of applied voltage.

LC-filled photonic crystal fiber

Photonic crystal fiber (PCF) is a polymer or glass fiber with an array of tiny air holes running along the length of the fiber. The waveguide properties of such fibers can be controlled by filling the air holes with additional material [13, 18–21]. The refractive index of LC can be easily tuned by electric field or temperature, therefore LC is suitable for this purpose. The technique of light reconfigurable alignment of LC in glass micro-tubes and in PCF was developed (Fig. 4) [13, 18–21].

A fairly homogeneous alignment was verified by polarizing optical microscopy and Fourier-transform infrared spectroscopy (FTIR). Since the presented technique is based on properly developed photoalignment azo dye materials [22], it is a promising non-contact method of LC orientation in complicated photonic crystal structures. The order parameter S of LC was acquired from FTIR data, and the good quality of alignment was confirmed.

Moreover, LC-filled thin porous films are to be investigated for the purpose of practical applications in electrically controlled optical attenuators and polarization-insensitive optical switches [23, 24].

Switchable diffraction gratings

Remnant high-efficiency polarization gratings are produced in nematic LC cells by exposing the azo dye molecule layers deposited on the substrate, to “interfering” beams with opposite circular polarizations [25]. The diffraction pattern is controlled by an electric signal applied across the LC cell. Polarization gratings are suitable for electrically controlled detection and discrimination of polarized components of light. All molecules of LC tend to be reoriented to a uniform homeotropic state at high voltage, and the modulation of LC alignment in the cell is terminated. Applications in LC optical switches are being discussed.

A diffraction grating was proposed by periodically defining the liquid crystal director distribution to form alternating planar aligned (PA) and twist nematic (TN) regions in an LC cell sandwiched between two crossed polarizers. Both 1D and 2D diffraction gratings demonstrate the diffraction efficiency of the total 1st order up to 12.0% and 18.2%, respectively (Fig. 5), due to their different voltage-dependent transmittance and phase modulation. When voltage was applied, four characteristic states were achieved, and the intensity of the 1st order could be suppressed by approximately 2 orders within 0.3 Vp-p at the driving voltage <2.5 Vp-p.

A Dammann grating based on hybrid photoaligned dual-frequency nematic LCs was demonstrated in 2016 [26–28]. The configuration of the Dammann grating is comprised of two substrates, one of which is coated with the homeotropic alignment, and the other substrate provides a planar, patterned alignment with mutually orthogonal easy axes in every two adjacent alignment domains. The produced polarization-independent Dammann grating could generate an optical array with equal light intensity distribution, which was characterized by the low uniformity deviation of ~ 0.081 , diffraction efficiency of more than 58%, response time <1 ms, and low driving voltage of ~ 3 V/ μm (Fig. 6).

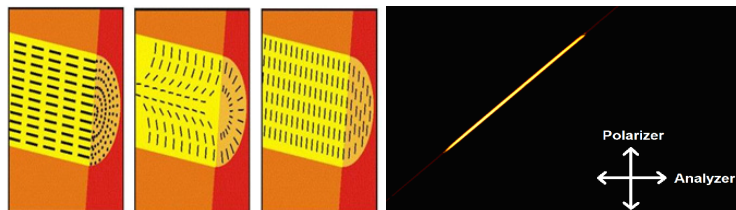


Fig. 4. Left to right: typical alignment of LC molecules in micro-capillary: planar, splay (axial, escaped radial), transverse; single-frame excerpt from a video recording of micro-capillaries filled with LC, in which two stable alignments (planar and tilted at 45°) have been obtained simultaneously [13, 21].

Optically rewritable technology for photonic devices

The ORW technology, pioneered in our research [12], can be successfully used for photonic applications. LC materials with optimized electro-optical properties provide a promising opportunity for application devices. As we know, there are no publications published by other groups on the application of optically rewritable technology for LC photonics devices. Several key devices have been developed, for example, light controllable LC plane waveguides, LC polarization-dependent elements, lenses and wave plates, LC polarization rotators and polarization controllers, light and voltage controllable diffraction gratings for optical filters, *etc.* One of such applications is shown in Fig. 7.

Using ORW photoalignment techniques, the smooth collimating refractive interface can be written by light in front of the waveguide immersed into LC (Fig. 6) [12]. The LC structure can be stabilized by the photoalignment layer without applied voltage. The *s*-polarized light can be coupled and it comes from the waveguide, going into a collimated beam inside the LC bulk for further processing, while the *p*-polarized light can be guided by matching polarization maintaining the LC waveguide [28]. We have developed a polarization-independent LC photonic device that can convert both polarization components, out-coupled from a polarization-independent waveguide to one polarization for further processing of light by a polarization-dependent LC structure for routing or other purposes. This new design

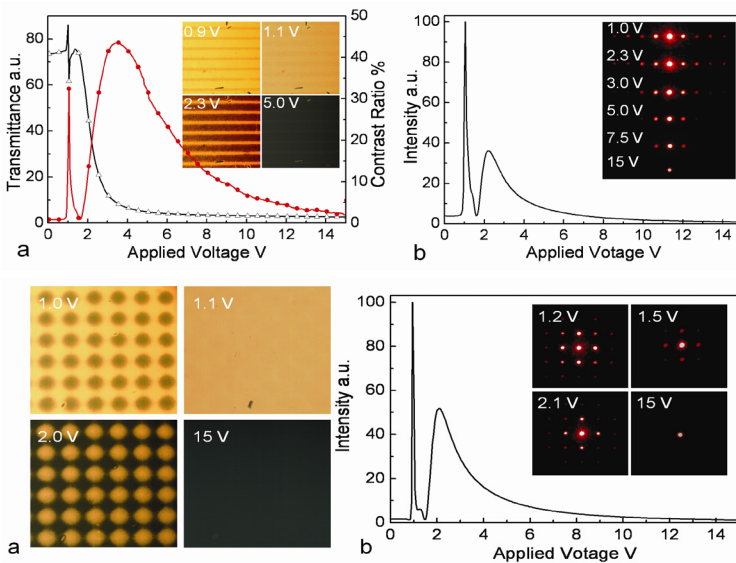


Fig. 5. Diffraction from periodically photoaligned homogeneous/twisted LC structures.

Top: LC switchable 1D diffraction grating.

- a) Transmittance–voltage curve (TVC) of the cell (*black line*) and contrast ratio between voltage-dependent intensity of the 1st and 0th orders (*red line*);
- b) intensity of the 1st order vs. driving voltage.

Bottom: LC switchable 2D diffraction grating.

- a) Four states of 2D TN-PA cell under different applied voltages;
- b) intensity of the 1st order vs. driving voltage.

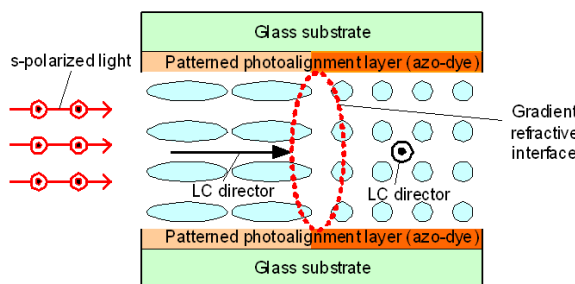


Fig. 7. Refractive interface for *s*-polarized light by nematic LC in the bulk of an LC cell [12].

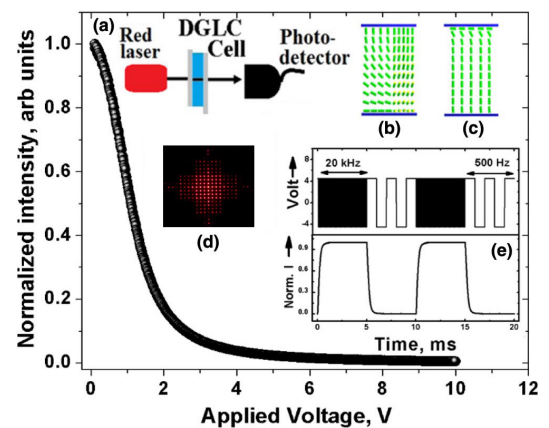


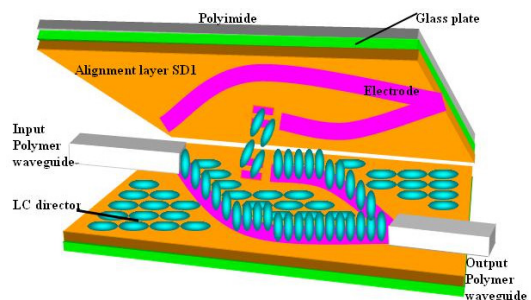
Fig. 6. Intensity vs. voltage curve (IVC) obtained by detection of light intensity of 1st order equal-intensity points.

(a) Experimental setup for measuring the IVC.

(b) Molecular alignment in the absence of an electric field; when a low-frequency high electric field was applied, the LC molecules were turned to the molecular state shown in (c).

(d) Diffraction pattern of the dual-frequency LC Dammann grating in the diffractive state.

(e) Electro-optical response of the Dammann grating (*bottom*) when a dual-frequency signal (*top*) was applied [26].



consists of polarization-maintaining LC waveguides, an LC polarization-dependent passive lens, and an active half-wave plate (HWP) [12].

Based on the outstanding ORW properties of the photoalignment material, a binary-phase LC circular Dammann grating, with two mutually orthogonal light-induced alignments in neighboring alignment domains, was proposed to generate annular patterns with an equal-intensity distribution in the far field [29]. A simple mask-free real-time optical tuning of the LC circular Dammann grating was achieved by mere control of the polarization of ultraviolet exposure light, as well as the energy dose, as shown in Fig. 8.

The proposed LC circular Dammann gratings with high efficiencies and desirable uniformities exhibited outstanding optical and electrical tunabilities.

Patterned micro-polarizer array with the photoalignment technology for image sensors

A thin patterned micro-polarizer array, generated by the photoalignment method for complementary metal-oxide-semiconductor (CMOS) image sensors, can be designed for the simultaneous detection of all four Stokes parameters of an output optical image (Fig. 9) [12]. A 2- μm pitch can be achieved by using UV light to rotate the four micro-polarizer elements. The experimental results have proved the concept

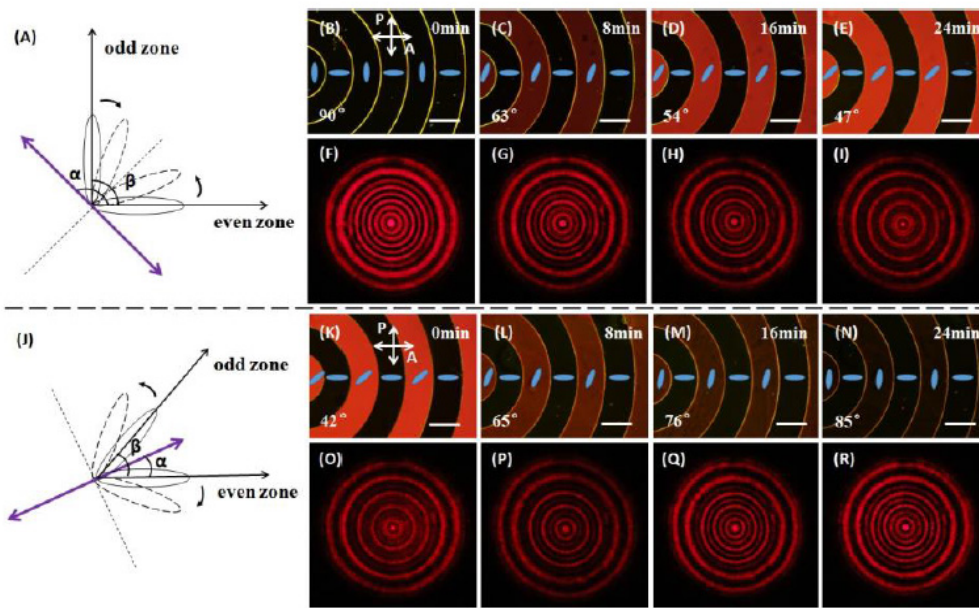


Fig. 8. Schematic diagrams of optical tuning of the β angle between the alignments in even zones and odd zones, micrographs under crossed polarizers, and corresponding diffraction patterns. Scale bars represent 200 μm . Respective optical tuning process for (A) reducing and (J) enlarging the β angle between the LC directors in even zones and odd zones by using linearly polarized UV light (denoted by purple double-headed arrow). (B–E) Micrographs for angle β , decreasing from 90° to 47° , with the increasing exposure time. (F–I) Corresponding diffraction patterns with even diffraction orders fading out. (K–N) Micrographs for angle β , increasing from 42° to 85° , with the increasing exposure time. (O–R) Corresponding diffraction patterns with even diffraction orders fading in [29].

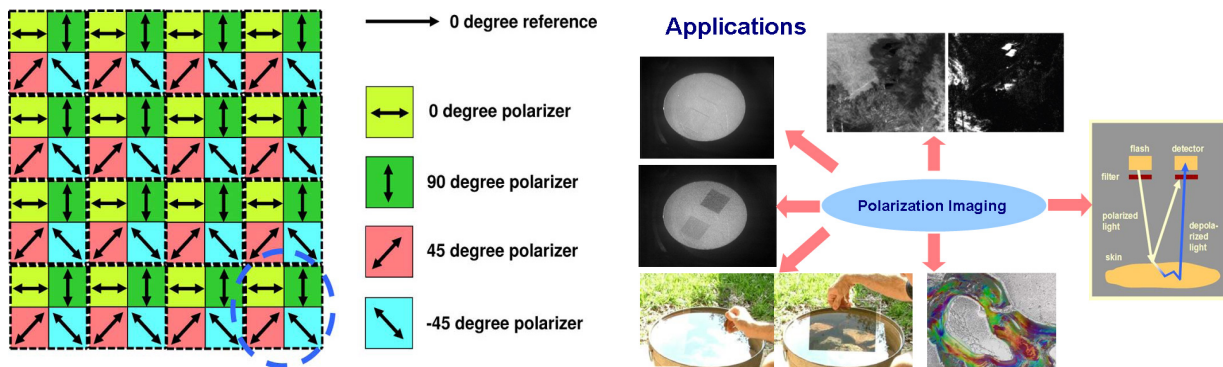


Fig. 9. Patterned micro-polarizer array for complementary metal-oxide-semiconductor (CMOS) image sensors with simultaneous detection of all four Stokes parameters of an output optical image, including “invisible objects” (constant transmission or reflection and no color) [12].

of high-performance photoaligned LC micro-polarizer arrays, with a high transmittance of $\sim 80\%$ and extinction ratio as high as ~ 3200 (35 dB).

The micro-polarizer array technology with a high transmittance and extinction ratio, exploiting the “guest–host” LC mode, can be used for visible imaging polarimetry [12, 30]. This high-resolution thin micro-polarizer array, with a $5 \times 5 \mu$ pixel pitch and 0.95μ thickness, was made by the “host” nematic LC molecules, photoaligned by the sulfonic azo dye SD1. The averaged major principal transmittance, polarization efficiency, and order parameter are 80.3%, 0.863, and 0.848, respectively, for the 400–700 nm spectral range. The proposed production technology completely removes the need for any selective etching during the manufacturing/integration process of the micro-polarizer array. It is fully CMOS-compatible, simple, and cost-effective, requiring only spin-coating followed by a single ultraviolet exposure through a “photoalignment master.” It is well adjusted for low-cost polarization imaging applications.

Electrically tunable liquid crystal q-plates

The photoalignment technology is used to create LC q-plates, tuned by electricity with various topological charges for generating optical vortex beams with definite orbital angular momentum (OAM) per photon [31–34]. Several tests have been conducted on the q-plates, including OAM tomography, showing excellent optical performance. These devices can be used in general and quantum optics. The azo dye materials showed a very high-resolution capability of LC alignment in these experiments (Fig. 10).

Electrically switchable liquid crystal Fresnel lens

A LC Fresnel lens based on alternate TN and PA regions (Fig. 11) was made by a two-step photoalignment process [35–38]. The LC Fresnel lens manifested two identical focal lengths because of the TN and PA alignment domains, giving rise to

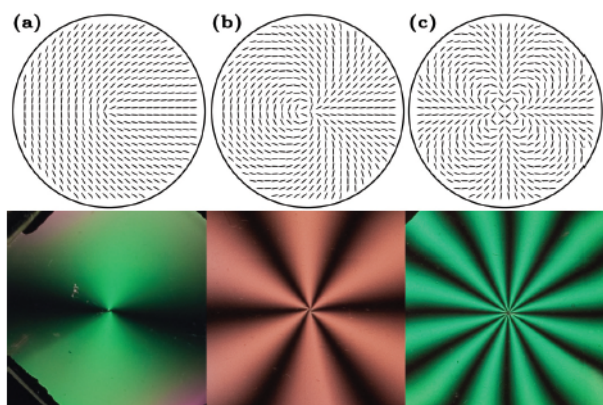


Fig. 10. LC pattern tunable q-plates made by photoalignment with high resolution [33].

the double light intensity at the focal point, and thus offered double efficiency of the conventional Fresnel zone plates.

A method of production of a LC Fresnel lens, based on a single alignment layer with patterned planar-aligned regions, was disclosed by Xiaoqian Wang *et al.* [39]. The binary-phase LC Fresnel lens demonstrated a diffraction efficiency of 39% at the focal point. Due to the mutually orthogonal alignment in neighboring domains (Fig. 12), the lens is polarization-independent, which is indeed a merit in the viewpoint of efficient energy use.

A polarization-independent Fresnel lens, based on a patterned hybrid aligned nematic dual-frequency LC, was demonstrated [40]. The LC Fresnel lens was made by assembling two glass substrates with different alignment materials. One substrate was coated with a homeotropic alignment layer, and the other was coated with an in-plane patterned alignment layer, wherein the easy axes in every two adjacent alignment domains were mutually orthogonal, as shown in Fig. 13. Due to the outstanding electro-optical properties of the dual-frequency LC, the proposed Fresnel lens exhibited fast-switching time under alternate high frequency and low-frequency electric fields.

Liquid crystal optical elements with integrated Pancharatnam–Berry phases

A polarization-dependent diffractive bifocal vortex lens based on the Pancharatnam–Berry phase was experimentally demonstrated [41–46]. The phase expression of the Pancharatnam–Berry phase optical vortex lens (PBOVL) comprised of two terms, i.e., a Pancharatnam–Berry lens term and a q-plate term. The non-separable spin angular momentum (SAM) and OAM photon states were established when an incident beam passed through the PBOVL, as shown in Fig. 14. Different OAM states at the output of

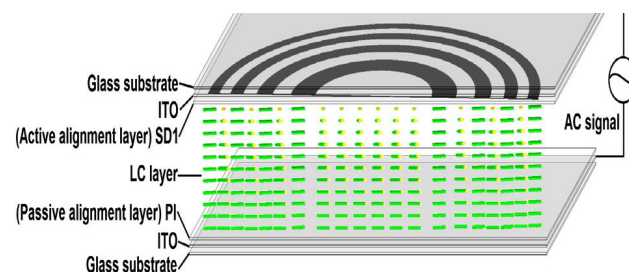


Fig. 11. Configuration of the LC Fresnel lens based on alternate TN and PA regions. One indium tin oxide coated glass substrate was coated with a polyimide layer, while the other substrate was coated with a photoalignment (SD1) layer. The white and black regions represent the TN and PA domains, respectively [35].

the PBOVL could be sorted by the bifocality of the manufactured lens. By using the underlying physics of the Pancharatnam–Berry phase polarization holography, the device was facilely, efficiently, and economically realized. The transmittance and diffraction efficiency of the device was 90% and 91%, respectively.

A LC Pancharatnam–Berry axilens was produced via a digital micro-mirror device (DMD)-based photopatterning system [47]. The polarization-dependent device behaved as an anti-axilens for RHC polarized incident light, for which an optical ring gradually expanded in the transverse direction at the output, and it acted as the axilens for LHC polarized incident light, for which an optical ring was focused with a long focal depth at the output. The modification of the size and sharpness of the diffracted hollow beam was demonstrated by encoding a positive (negative) PB lens term into the director orientation expression of a PB (anti-)axicon, as shown in Fig. 15.

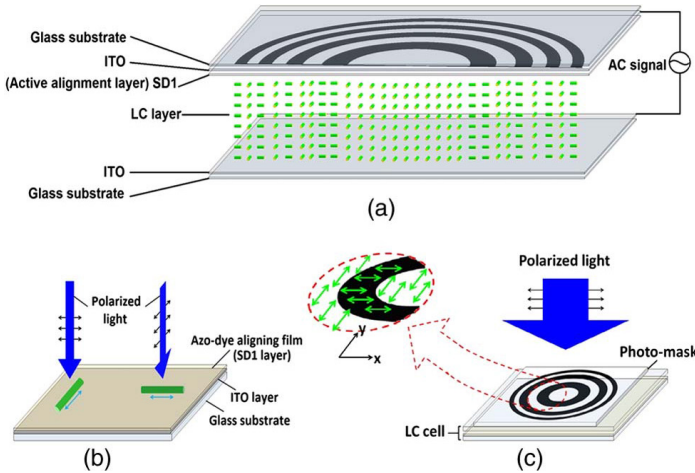


Fig. 12. (a) Configuration of liquid crystal Fresnel lens. (b) Schematic of photoalignment process. The SD1 molecules aligned perpendicular to the polarization of the incident light after sufficient exposure dosage. (c) Photopatterning process with an amplitude photomask. The magnified area in the red dashed circle represents the easy axis distribution in two different alignment domains [39].

A LC beam-splitting lens was made, with spatially separated focuses via the LC photoalignment technology [48–50]. The proposed lens with exotic optical properties was created by integrating a polarization grating with a Pancharatnam–Berry phase LC lens. The two focuses of the proposed lens, i.e., $+f$ and $-f$, could be spatially separated (Fig. 16). When a linearly polarized incident light successively passed through a conventional convex glass lens with a proper focal length and the fabricated lens, the two emergent light beams exhibited convergent optical behavior and the two focuses were spatially separated. Moreover, by adjusting the distance between the proposed lens and the conventional glass lens, the focal lengths of the lens system could be modulated.

FAST FERROELECTRIC LCD

The ferroelectric liquid crystal (FLC) is the fastest LC mode, which can work with fast-response time and low driving voltages, and is highly suitable for field

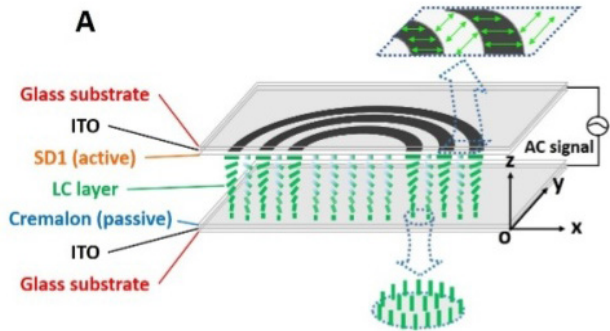


Fig. 13. Configuration of hybrid aligned nematic dual-frequency liquid crystal Fresnel lens. The SD1 molecules under black regions (even zones) and white regions (odd zones) orient in the $X-O-Z$ plane and the $Y-O-Z$ plane, respectively. The magnified area in the blue dashed square depicts the easy axis distribution in two different alignment domains, and the area in the blue dashed circle represents the homeotropic alignment of LC molecules [40].

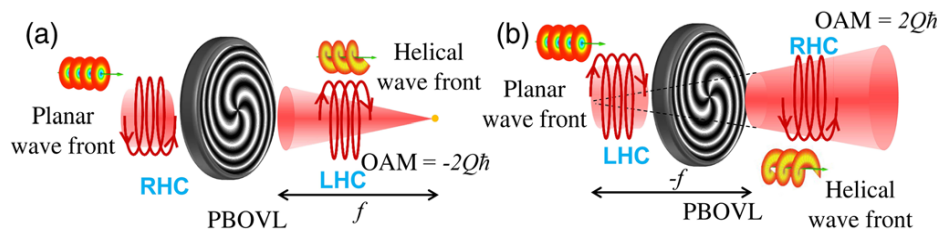


Fig. 14. Coupling of SAM-OAM states at the output of the PBOVL. (a) For the right-handed circularly (RHC) polarized incident beam, each photon of the focusing output beam possessed an OAM of $-2Q\hbar$ and was left-handed circularly (LHC) polarized with a corresponding SAM of $+\hbar$. (b) For the LHC polarized incident beam, each photon of the defocusing output beam possessed an OAM of $+2Q\hbar$ and was RHC polarized with a corresponding SAM of $-\hbar$ [41].

sequential applications [12, 51–55]. Fast-switching ferroelectric liquid crystal displays (FLCD) have the potential to become the new generation of the field sequential color (FSC) LCD, which is proved to have a better response time than the usual nematic LC. The best FLC parameters can be obtained on the basis of electrically suppressed helix mode [12].

A reflective display cell has been proposed—suitable for projection displays based on electrically suppressed helix ferroelectric liquid crystal (ESHFLC) with a fast-response time, which is quite suitable for the field sequential display [56, 57]. The pulse width modulation technique is used to control the residual light and provide several grey levels.

The electro-optical performance of the reflective cell at the electric field of 3 V and frequency of 5 kHz was set to achieve a high number of colors.

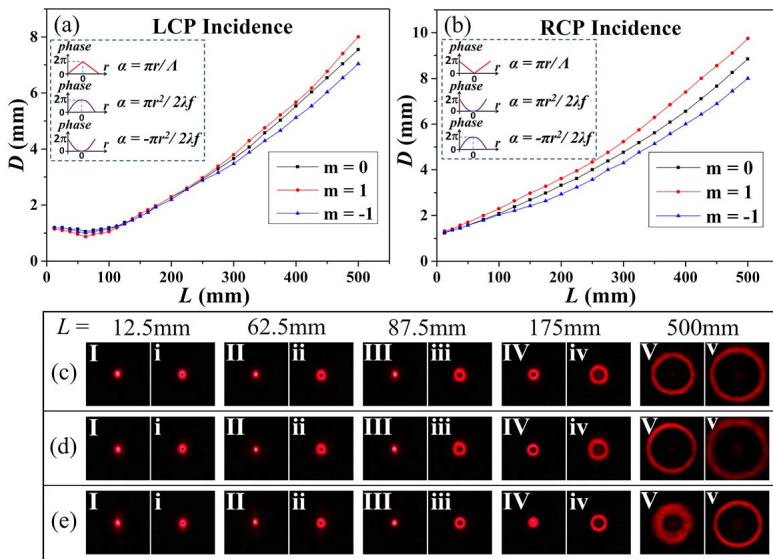


Fig. 15. Comparison of the diffraction properties of three PB axilenses (PBALs). Diagrams of the diffracted ring diameter (D) vs. propagation distance (L) for three PBALs under (a) the left-handed circularly polarized (LCP) and (b) the right-handed circularly polarized (RCP) incident beams. The inserts in (a) and (b) show mutually reversed phase profiles for the corresponding director distributions under different circularly polarized beams. The diffraction patterns for (c) PBAL-I ($m = 0$), (d) PBAL-II ($m = 1$), and (e) PBAL-III ($m = -1$) under (I–V) LCP and (i–v) RCP incident beams at representative distances [47].

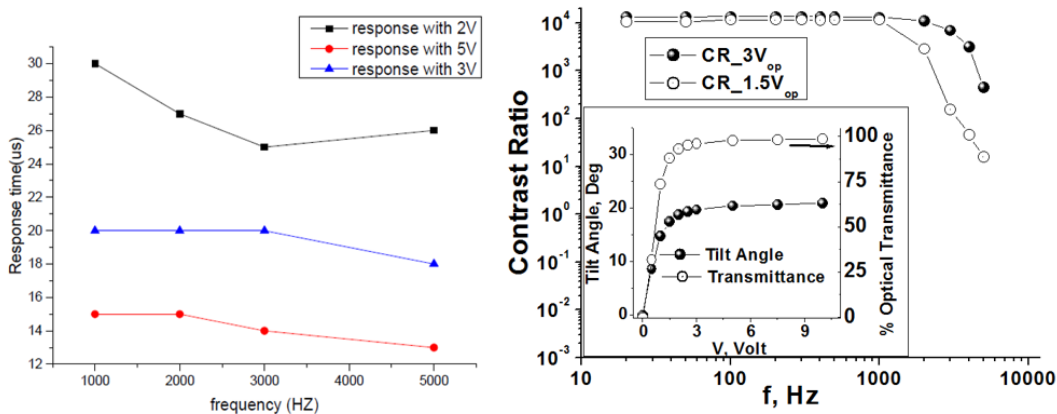


Fig. 17. Left: response time vs. driving frequency at different driving voltages [56]. Right: electro-optical response of the photoaligned ESHFLC [12].

The response time vs. the driving frequency, at different driving voltages, is shown in Fig. 17. Even at small driving voltages, the reflective FLC cell still maintains the contrast ratio (CR) enough for the display, $CR > 10000 : 1$. The response time of the reflective FLC cell at 5 kHz and the electric field of 5 V was around 14 μ s. Such a fast-response time allows us to drive the FLC cell even at a very high frequency of 5 kHz (Fig. 17).

Novel photoaligned FLC devices may include FSC FLC with a high resolution, low power consumption and extended color gamut, which can be used in the screens of portable computers, mobile phones, personal digital assistants. The switchable goggles and lenses based on new FLC prototypes can be efficiently applied in the new generations of switchable 2D/3D LCD TV. The FSC FLC micro-display, which is one

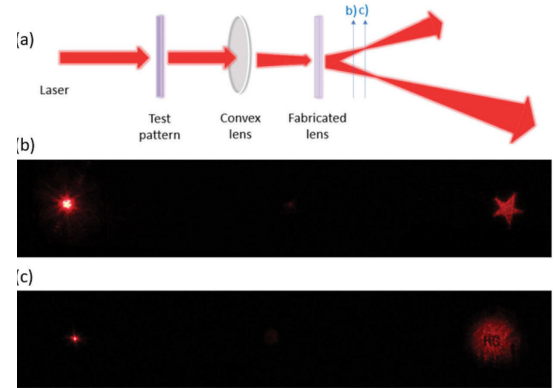


Fig. 16. (a) Schematic optical setup of the system with a screen placed at position (b) when a pentagram is used as the test pattern and (c) when the test pattern is changed to the letters “HG” [48].

of the most advanced technologies for pico-projectors, can be also made on the basis of new materials and electro-optical modes in FLC [12]. The photoalignment technology enables to solve the key problems usually faced in FLC applications, such as (i) quality of FLC alignment on sufficiently large surface area; (ii) appropriate adjustable anchoring energy and pretilt angle; (iii) low loss in the alignment layers due to their small thickness, *etc.* [12].

Future development of novel photoaligned fast FSC FLC is aimed at: (i) further fundamental study of the new appropriate electro-optical modes used for switching; (ii) better understanding of the physical mechanisms of FLC interaction with a photoaligned surface of different photosensitive nature to produce a stable alignment with a controllable anchoring energy and pretilt angle over a sufficiently large surface area; (iii) development of new fast-response FLC materials with fast switching and a sufficient number of switchable grey levels (V-shape switching); (iv) implementation of the working prototypes of novel FSC FLC displays; (v) investigation of operation modes to allow the use of efficient addressing of FLC.

CONCLUSIONS

The LC photoalignment and photopatterning technology for new display and photonic applications

REFERENCES

1. Ichimura K. Photoalignment of Liquid-Crystal Systems. *Chem. Rev.* 2000;100(5):1847-1873. <https://doi.org/10.1021/cr980079e>
2. Schadt M., Seiberle H., Schuster A. Optical patterning of multidomain liquid-crystal displays with wide viewing angles. *Nature.* 1996;381(6579):212-215. <https://doi.org/10.1038/381212a0>
3. O'Neill M., Kelly S.M. Photoinduced surface alignment for liquid crystal display. *J. Phys. D: Appl. Phys.* 2000;33(10):R67-R84. <https://doi.org/10.1088/0022-3727/33/10/201>
4. Gibbons W.M., Shannon P.J., Sun S.-T., Swetlin B.J. Surface-mediated alignment of nematic liquid crystals with polarized laser light. *Nature.* 1991;351(6321):49-50. <https://doi.org/10.1038/351049a0>
5. Chatelain P. Sur l'orientation des cristaux liquides par les surfaces frottées. *Bulletin de Minéralogie.* 1943;66(1-6):105-130 (in French). <https://doi.org/10.3406/bulmi.1943.4528>
6. Janning J.L. Thin film surface orientation for liquid crystals. *Appl. Phys. Lett.* 1972;21(4):173-174. <https://doi.org/10.1063/1.1654331>
7. Chigrinov V.G., Kozenkov V.M., Kwok H.S. *Photoalignment of Liquid Crystalline Materials: Physics and Applications.* Wiley; 2008. 248 p.
8. Yaroshchuk O., Reznikov Y. Photoalignment of liquid crystals: Basics and current trends. *J. Mater. Chem.* 2012;22(2):286-300. <https://doi.org/10.1039/C1JM13485J>
9. Nishikawa M., Taheri B., and West J.L. Mechanism of unidirectional liquid-crystal alignment on polyimides with linearly polarized ultraviolet light exposure. *Appl. Phys. Lett.* 1998;72:2403-2405. <https://doi.org/10.1063/1.121390>
10. Gong S., Kanicki J., Ma L., Zhong J. Ultraviolet-light induced liquid-crystal alignment on polyimide films. *Jpn. J. Appl. Phys.* 1999;38:5996-6004. <https://doi.org/10.1143/JJAP.38.5996>
11. Dyadyusha A.G., Marusii T.Ya., Reznikov Yu.A., Khizhnyak A.I., Reshetnyak V.Yu. Orientational effect due to a change in the anisotropy of the interaction between a liquid crystal and a bounding surface. *JETP Lett.* 1992;56:17-21.
12. Chigrinov V.G., Kwok H.S. *Photoalignment of liquid crystals: applications to fast response ferroelectric liquid crystals and rewritable photonic devices.* In: *Progress in Liquid Crystal Science and Technology: in Honor of Shunsuke Kobayashi's 80th Birthday.* Singapore: World Scientific; 2013. p. 199-226. https://doi.org/10.1142/9789814417600_0009
13. Chigrinov V.G. *Liquid Crystal Photonics.* Nova Science Publishers; 2014. 204 p. ISBN: 978-1-62948-315-3
14. Xu P., Chigrinov V., Kwok H.S. Optical analysis of a liquid-crystal switch system based on total internal reflection. *J. Opt. Soc. Am. A.* 2008;25(4):866-873. <https://doi.org/10.1364/JOSAA.25.000866>
15. Muravsky A., Chigrinov V. *Optical switch based on nematic liquid crystals.* IDW'05 Digest; 2005. 223 p.
16. Maksimochkin A.G., Pasechnik S.V., Tsvetkov V.A., Yakovlev D.A., Maksimochkin G.I., Chigrinov V.G. Electrically controlled switching of light beams in the plane of liquid crystal layer. *Opt. Commun.* 2007;270:273-279. <https://doi.org/10.1016/j.optcom.2006.09.014>

is a prominent research area. Such elements have started to appear in displays and on the photonics market. The electro-optical modes are used for light polarization rotation, voltage controllable diffraction, and fast switching of the LC refractive index. The photoalignment technique makes it possible to develop new LC fiber components. Photo-aligning materials are used to align LC in super-thin photonic holes, curved and 3D surfaces, and as cladding layers in micro-ring silicon-based resonators. The prototypes of new efficient LC photonic devices, such as optically rewritable LC E-paper, waveguides, and voltage controllable diffraction gratings are envisaged. The polarization controllers, polarization rotators, VOA, and other passive LC optical elements for fiber communication networks are in development.

We hope that this review can be interesting not only to a wide range of engineers, scientists, and managers, who are willing to develop new LC displays or other LC photonic devices and optical components, but also to researchers in other practically important fields, where the formation of new highly-ordered structures of organic molecules is desirable.

Автор заявляет об отсутствии конфликта интересов.

The author declares no conflicts of interest.

17. Zhuang Z., Suh S.W., Patel J.S. Polarization controller using nematic liquid crystals. *Opt. Lett.* 1999;24:694. <https://doi.org/10.1364/OL.24.000694>
18. Ertman S., Srivastava A.K., Chigrinov V.G., Chychłowski M.S., Woliński T.R. Patterned alignment of liquid crystal molecules in silica micro-capillaries. *Liq. Cryst.* 2013;40(1):1-6. <https://doi.org/10.1080/02678292.2012.725869>
19. Du F., Lu Y.-Q., Wu S.-T. Electrically tunable liquid-crystal photonic crystal fiber. *Appl. Phys. Lett.* 2004;85(12):2181-2183. <https://doi.org/10.1063/1.1796533>
20. Haakestad M.W., Alkeskjold T.T., Nielsen M.D., Scolari L., Riishede J., Engan H.E., Bjarklev A. Electrically tunable photonic bandgap guidance in a liquid-crystal-filled photonic crystal fiber. *IEEE Photonic. Tech. L.* 2005;17(4):819-821. <https://doi.org/10.1109/LPT.2004.842793>
21. Scolari L., Alkeskjold T.T., Riishede J., Bjarklev A., Hermann D.S., Anawati, Nielsen M.D., Bassi P. Continuously tunable devices based on electrical control of dual-frequency liquid crystal filled photonic bandgap fibers. *Opt. Express.* 2005;13(19):7483-7496. <https://doi.org/10.1364/OPEX.13.007483>
22. Valyukh I., Arwin H., Chigrinov V., Valyukh S. UV-induced in-plane anisotropy in layers of mixture of the azo-dyes SD-1/SDA-2 characterized by spectroscopic ellipsometry. *Phys. Status Solidi C.* 2008;5(5):1274-1277. <https://doi.org/10.1002/pssc.200777881>
23. Cimrova V., Neher D., Hilderbrandt R., Hegelich M., von der Lieth A., Marowsky G., Hagen R., Kostromine S., Bieringer T. Comparison of the birefringence in an azobenzene-side-chain copolymer induced by pulsed and continuous-wave radiation. *Appl. Phys. Lett.* 2002;81:1228. <https://doi.org/10.1063/1.1499766>
24. Kiselev A.D., Pasechnik S.V., Shmeliova D.V., Chopik A.P., Semerenko D.A., Dubtsov A.V. Waveguide Propagation of Light in Polymer Porous Films Filled with Nematic Liquid Crystals. *Advances in Condensed Matter Physics.* 2019;1539865. <https://doi.org/10.1155/2019/1539865>
25. Presnyakov V., Asatryan K., Galstian T., Chigrinov V. Optical polarization grating induced liquid crystal microstructure using azo-dye command layer. *Opt. Express.* 2006;14:10558-10564. <https://doi.org/10.1364/OE.14.010558>
26. Wang X.Q., Srivastava A.K., Fan F., Zheng Z.G., Shen D., Chigrinov V.G., Kwok H.S. Electrically/optically tunable photo-aligned hybrid nematic liquid crystal Damman grating. *Opt. Lett.* 2016;41:5668-5671. <https://doi.org/10.1364/OL.41.005668>
27. Luo D., Dai H.T., Sun X.W. Polarization tunable circular Damman grating generated from azo-dye doped nematic liquid crystals. *Proceedings of SPIE.* 2011;7934:79340H. <https://doi.org/10.1117/12.874139>
28. Luo D., Sun X.W., Dai H.T., Demir H.V. Polarization-dependent circular Damman grating made of azo-dye-doped liquid crystals. *Appl. Opt.* 2011;50(15):2316-2321. <https://doi.org/10.1364/AO.50.002316>
29. Wang X., Wu S., Yang W., Yuan C., Li X., Liu Z., Tseng M., Chigrinov V.G., Kwok H., Shen D., Zheng Z. Light-Driven Liquid Crystal Circular Damman Grating Fabricated by a Micro-Patterned Liquid Crystal Polymer Phase Mask. *Polymers.* 2017;9:380. <https://doi.org/10.3390/polym9080380>
30. Zhao X., Bermak A., Boussaid F. A low cost CMOS polarimetric ophthalmoscope scheme for cerebral malaria diagnostics. *IFIP Advances in Information and Communication Technology.* 2012;379 AICT:1-9. https://doi.org/10.1007/978-3-642-32770-4_1
31. Slussarenko S., Murauski A., Du T., Chigrinov V., Marrucci L., Santamato E. Tunable liquid crystal q-plates with arbitrary topological charge. *Opt. Express.* 2011;19(5):4085-4090. <https://doi.org/10.1364/OE.19.004085>
32. Wei B.-Y., Liu S., Chen P., Qi S.-X., Zhang Y., Hu W., Lu Y.-Q., Zhao J.-L. Vortex Airy beams directly generated via liquid crystal q-Airy-plates. *Appl. Phys. Lett.* 2018;112(12):121101. <https://doi.org/10.1063/1.5019813>
33. Aizawa M., Ota M., Hisano K., Akamatsu N., Sasaki T., Barrett C.J., Shishido A. Direct fabrication of a q-plate array by scanning wave photopolymerization. *J. Opt. Soc. Am. B: Optical Physics.* 2019;36(5):D47-D51. <https://doi.org/10.1364/JOSAB.36.000D47>
34. Huang Y.-H., Li M.-S., Fuh A.Y.-G. The application of liquid crystal q-plates for modulating Gaussian Beam. *Proceedings of the International Display Workshops.* 2013;1:196-197.
35. Wang X., Srivastava A., Chigrinov V., Kwok H. Switchable Fresnel lens based on micropatterned alignment. *Opt. Lett.* 2013;38:1775-1777. <https://doi.org/10.1364/OL.38.001775>
36. Lin L.-C., Jau H.-C., Lin T.-H., Fuh A.Y.-G. Highly efficient and polarization-independent Fresnel lens based on dye-doped liquid crystal. *Opt. Express.* 2007;15(6):2900-2906. <https://doi.org/10.1364/OE.15.002900>
37. Lin L.-C., Cheng K.-T., Liu C.-K., Ting C.-L., Jau H.-C., Lin T.-H., Fuh A.Y.-G. Fresnel lenses based on dye-doped liquid crystals. *Proceedings of SPIE.* 2008;6911:69110I. <https://doi.org/10.1117/12.762550>
38. Huang Y.-H., Huang S.-W., Chu S.-C., Fuh Y.-G. High-efficiency Fresnel lens fabricated by axially symmetric photoalignment method. *Appl. Optics.* 2012;51(32):7739-7744. <https://doi.org/10.1364/AO.51.007739>
39. Wang X.Q., Fan F., Du T., Tam A.M., Ma Y., Srivastava A.K., Chigrinov V.G., Kwok H.S. Liquid crystal Fresnel zone lens based on single-side-patterned photoalignment layer. *Appl. Opt.* 2014;53:2026-2029. <https://doi.org/10.1364/AO.53.002026>
40. Wang X.Q., Yang W.Q., Liu Z., Duan W., Hu W., Zheng Z.G., Shen D., Chigrinov V.G., Kwok H.S. Switchable Fresnel lens based on hybrid photo-aligned dual frequency nematic liquid crystal. *Opt. Mater. Express.* 2017;7:8-15. <https://doi.org/10.1364/OME.7.000008>
41. Tam A.M.W., Fan F., Du T., Hu W., Zhang W., Zhao C., Wang X., Ching K.L., Li G., Luo H., Chigrinov V.G., Wen S., Kwok H.S. Bifocal Optical-Vortex Lens with Sorting of the Generated Nonseparable Spin-Orbital Angular-Momentum States. *Phys. Rev. Applied.* 2017;7:034010. <https://doi.org/10.1103/PhysRevApplied.7.034010>
42. Duan W., Chen P., Ge S.-J., Wei B.-Y., Hu W., Lu Y. Helicity-dependent forked vortex lens based on photo-patterned liquid crystals. *Opt. Express* 2017;25(13):14059-14064. <https://doi.org/10.1364/OE.25.014059>
43. He Z., Lee Y.-H., Chen R., Chanda D., Wu S.-T. Switchable Pancharatnam-Berry microlens array with nano-imprinted liquid crystal alignment. *Opt. Lett.* 2018;43(20):5062-5065. <https://doi.org/10.1364/OL.43.005062>

44. Zhan T., Xiong J., Lee Y.-H., Wu S.-T. Polarization-independent Pancharatnam-Berry phase lens system. *Opt. Express*. 2018;26(26):35026-35033. <https://doi.org/10.1364/OE.26.035026>
45. Duan W., Chen P., Ge S.-J., Liang X., Hu W. A fast-response and helicity-dependent lens enabled by micro-patterned dual-frequency liquid crystals. *Crystals*. 2019;9(2):111. <https://doi.org/10.3390/cryst9020111>
46. Li S., Liu Y., Li Y., Liu S., Chen S., Su Y. Fast-response Pancharatnam-Berry phase optical elements based on polymer-stabilized liquid crystal. *Opt. Express*. 2019;27(16):22522-22531. <https://doi.org/10.1364/OE.27.022522>
47. Ren J., Wang W., Yang W., Yuan C., Zhou K., Li X., Tam A.M., Meng C., Sun J., Chigrinov V., Kwok H., Wang X., Zheng Z., Shen D. Micro-patterned liquid crystal Pancharatnam-Berry axilens. *Chin. Opt. Lett.* 2018;16:062301. <https://www.osapublishing.org/col/abstract.cfm?uri=col-16-6-062301>
48. Zhou Y., Yin Y., Yuan Y., Lin T., Huang H., Yao L., Wang X., Tam A.M.W., Fan F., Wen S. Liquid crystal Pancharatnam-Berry phase lens with spatially separated focuses. *Liq. Cryst.* 2019;46(7):995-1000. <https://doi.org/10.1080/02678292.2018.1550820>
49. Ke Y., Liu Y., Zhou J., Liu Y., Luo H., Wen S. Optical integration of Pancharatnam-Berry phase lens and dynamical phase lens. *Appl. Phys. Lett.* 2016;108(10):101102. <https://doi.org/10.1063/1.4943403>
50. Chen H.-T., Taylor A.J., Yu N. A review of metasurfaces: Physics and applications. *Rep. Prog. Phys.* 2016;79(7):076401. <https://doi.org/10.1088/0034-4885/79/7/076401>
51. Lagerwall S.T. *Ferroelectric and Antiferroelectric Liquid Crystals*. Weinheim: Wiley-VCH; 1999.
52. Favalora G.E., Napoli J., Hall D.M., Dorval R.K., Giovinco M.G., Richmond M.J., Chun W.S. 100 million-voxel volumetric display. *Proceedings of SPIE*. 2002;4712:300-312. <https://doi.org/10.1117/12.480930>
53. Nagaraj M., Panarin Y.P., Manna U., Vij J.K., Keith C., Tschierske C. Electric field induced biaxiality and the electro-optic effect in a bent-core nematic liquid crystal. *Appl. Phys. Lett.* 2010;96(1):011106. <https://doi.org/10.1063/1.3280817>
54. Kim D.-W., Yu C.-J., Lim Y.-W., Na J.-H., Lee S.-D. Mechanical stability of a flexible ferroelectric liquid crystal display with a periodic array of columnar spacers. *Appl. Phys. Lett.* 2005;87(5):051917. <https://doi.org/10.1063/1.2007856>
55. Kumar A., Prakash J., Deshmukh A.D., Haranath D., Silotia P., Biradar A.M. Enhancing the photoluminescence of ferroelectric liquid crystal by doping with ZnS quantum dots. *Appl. Phys. Lett.* 2012;100(13):134101. <https://doi.org/10.1063/1.3698120>
56. Shi L., Ma Y., Srivastava A., Chigrinov V., Kwok H.S. *Field Sequential Color Displays based on Reflective Electrically Suppressed Helix Ferroelectric Liquid Crystal*. SID – 2015 International Symposium. 2015; San Jose, CA, USA.
57. Srivastava A.K., Shi L., Kwok H.S. Modern display applications based on ESH ferroelectric liquid crystals. *Proceedings of the International Display Workshops*. 2018;1:62-65.

About the author:

Vladimir G. Chigrinov, Dr. of Sci. (Physics), Professor, Honorary Member of the International Display Society, School of Physics and Optoelectronic Engineering, Foshan University (18, Jiang-Wan-Yi-Lu, Chancheng, Foshan, Guangdong, 528000, P.R. China). E-mail: eechigr@ust.hk. Scopus Author ID: 35601969500, ResearcherID: I-7648-2013, <https://orcid.org/0000-0003-0593-2555>

Об авторе:

Чигринов Владимир Григорьевич, доктор физико-математических наук, профессор, почетный член Международного дисплейного общества, Школа физики и оптоэлектронного инжиниринга, Фощаньский университет (18, Jiang-Wan-Yi-Lu, Chancheng, Foshan, Guangdong, 528000, P.R. China). E-mail: eechigr@ust.hk. Scopus Author ID: 35601969500, ResearcherID: I-7648-2013, <https://orcid.org/0000-0003-0593-2555>

Поступила: 23.01.2020; Получена после доработки: 28.02.2020; Принята к опубликованию: 10.04.2020.
Submitted: January 23, 2020; Reviewed: February 28, 2020; Accepted: April 10, 2020.